50 or 500?
Current Issues in Estimating Fault Rupture Length

SECTIONS

Los Angeles Times

SUBSCRIBE
4 weeks for 99¢

LOG IN

FRIDAY DEC. 2, 2016 | MOST POPULAR | LOCAL | SPORTS | ENTERTAINMENT | POLITICS | OPINION | PLACE AN AD | 64°

LOCAL / L.A. Now

A mega-quake stretching from L.A. to San Francisco would devastate California, with $289 billion in losses, study finds

David P. Schwartz
USGS Menlo Park

USGS
science for a changing world

Hire Tom Rockwell!

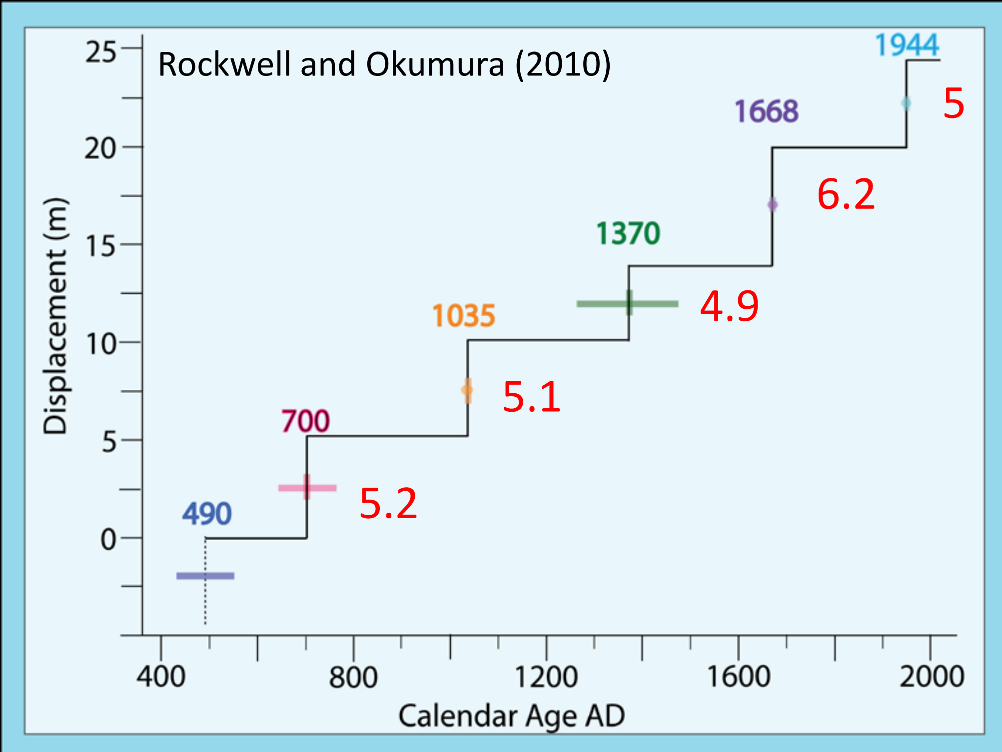

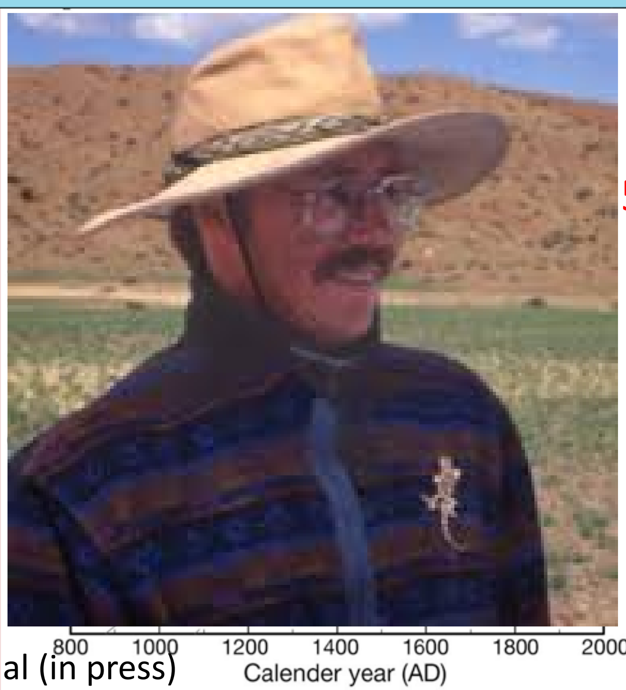

5

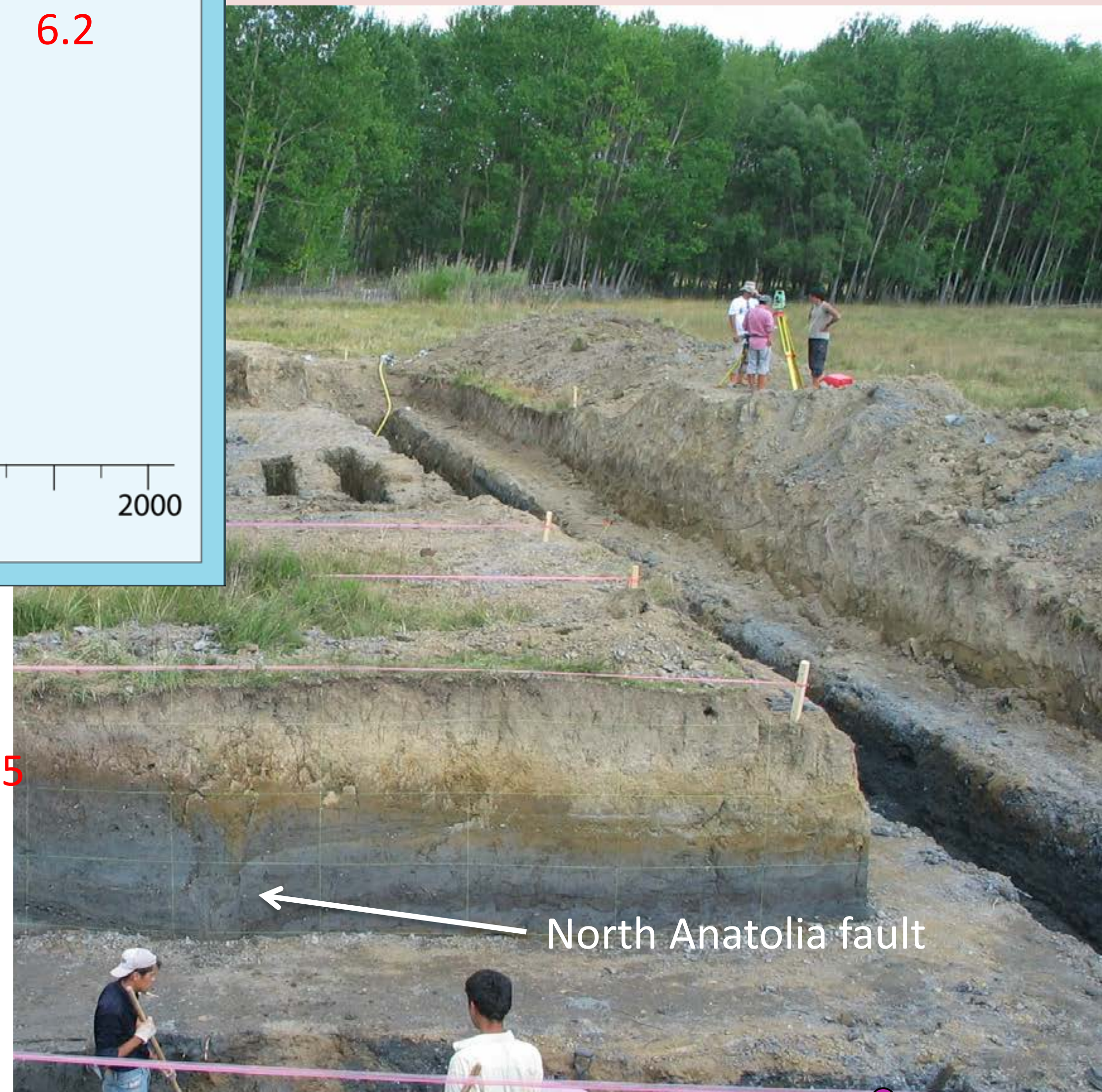

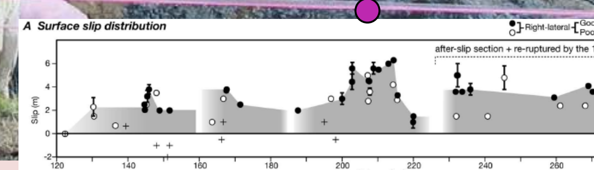

Kondo et al (in press)

Put Lloyd Cluff into Helicopter with Camera!

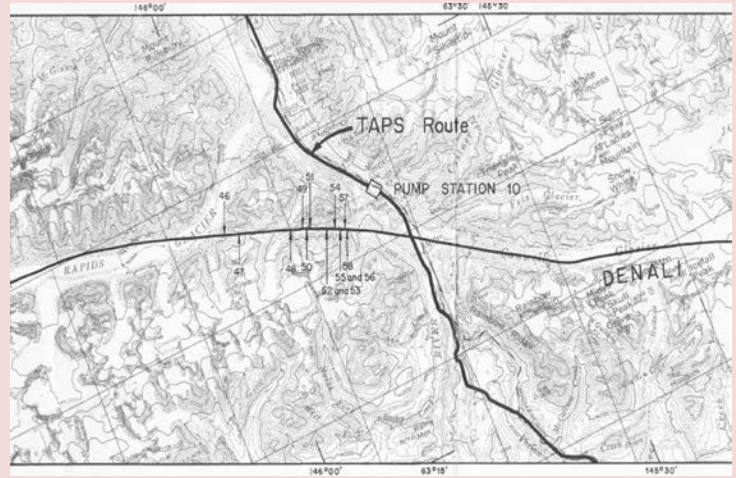

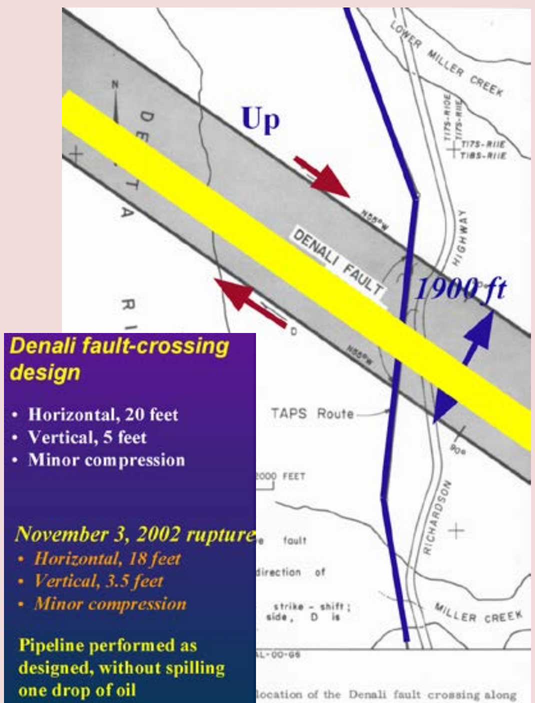

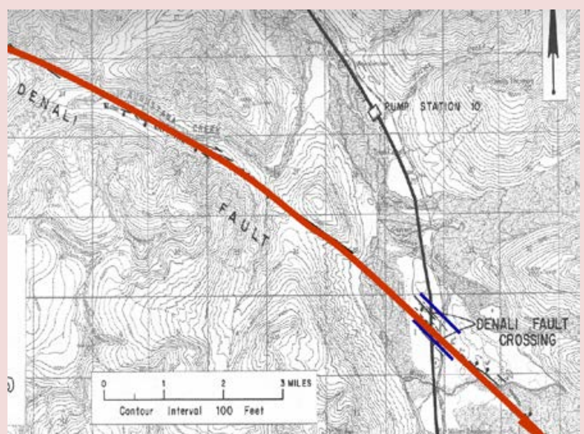

Why Length?

Fundamental parameter for estimates of Mw →

Scaling relations between Mw and D

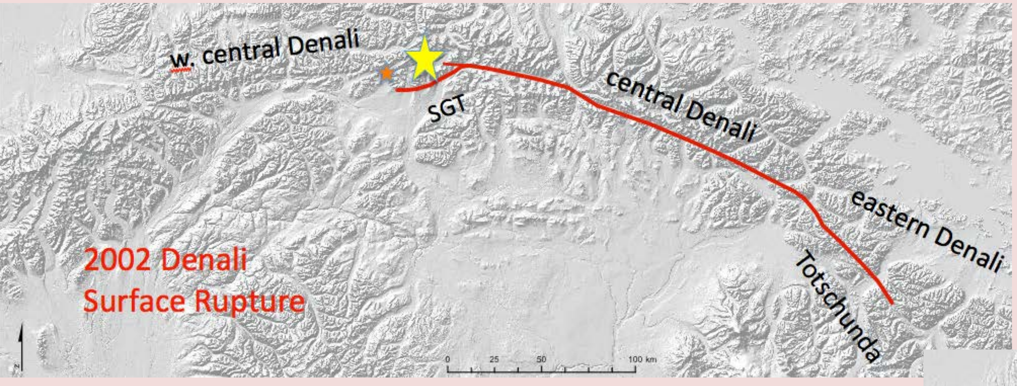

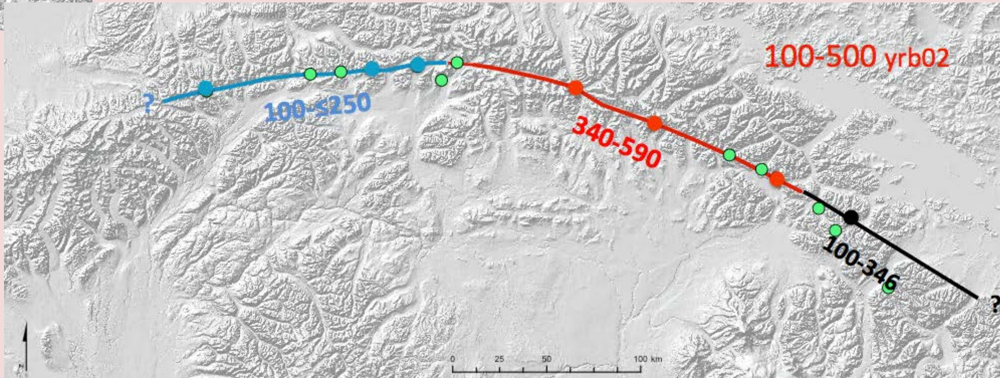

Rupture Length Issues
for Faults in Shallow Continental Crust

Segmentation (prescribed) vs relaxation of segmentation

Are faults, particularly longer zones, composed of ditinct, repeatable, rupture sources (segments)? Can these be identified prior to a rupture?

What is potential for multi-fault (as opposed to multi segment) rupture?

Are there preferential structural settings for segmentation to occur?

What are the differences in estimating length for different fault types?

To what degree do segmentation models proposed to date underestimate/overestimate the length of future ruptures?

What controls rupture length? Can more physics be incorporated?

Can segmentation models be tested?

WGCEP 88:

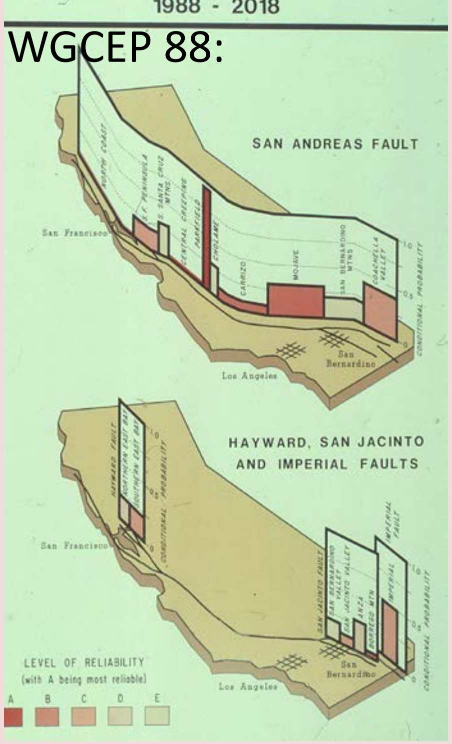

WGCEP 90

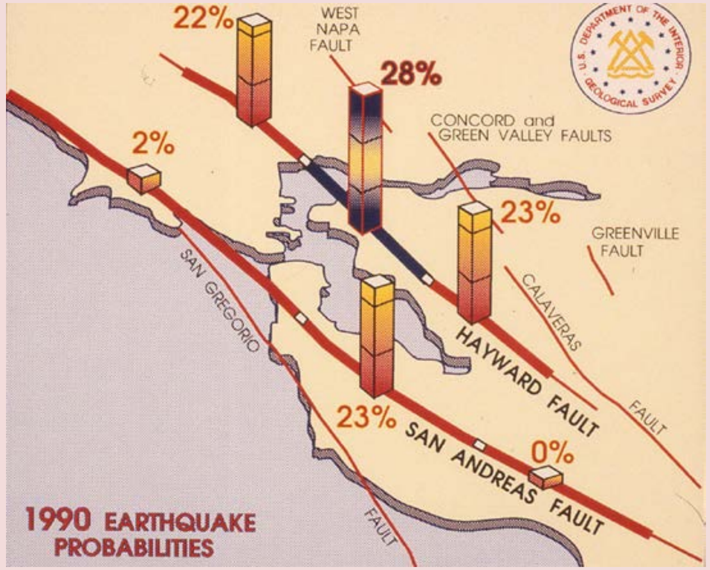

WGCEP 95

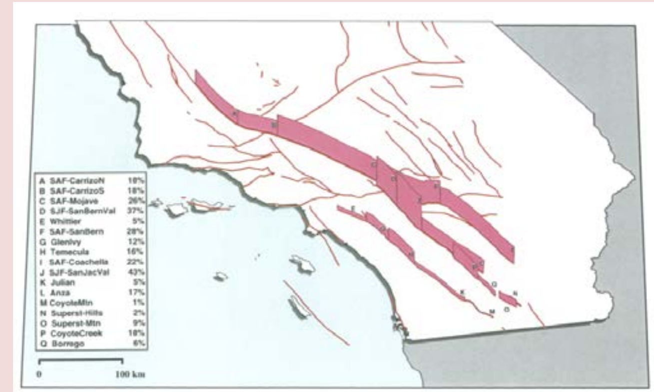

WGCEP 99/03

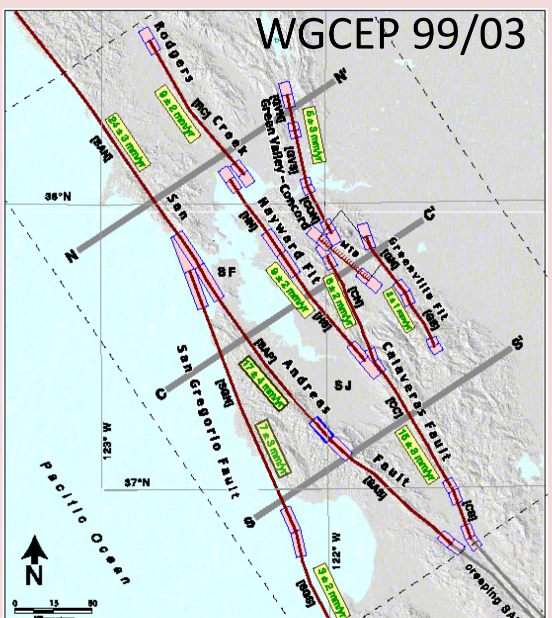

WGCEP 07: UCERF 2

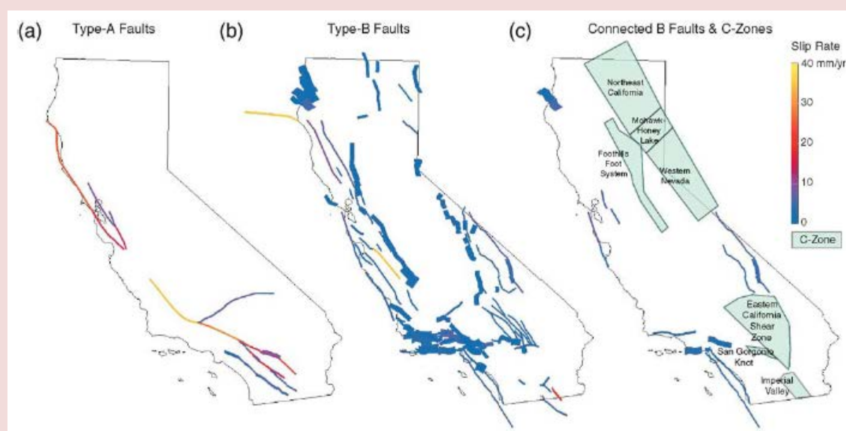

WGUEP

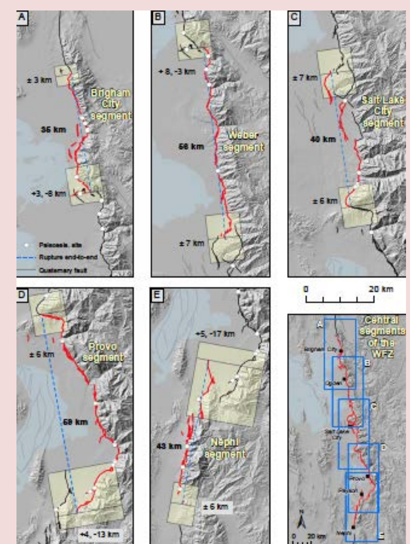

USGS
science for a changing world

Earthquake Probabilities in the San Francisco Bay Region: 2002–2031

By Working Group On California Earthquake Probabilities

Open-File Report 03-214

WGCEP 99/03

San Francisco Bay Region

Segmentation models based on **behavioral differences** (event timing, slip rate changes, transitions from locked to creeping, microseismicity distribution) and **kinematic variables** (steps, branch points, bends, changes in trace complexity)

Multi-segment ruptures (though not multi-fault)

Uncertainty in rupture endpoints, overlapping ruptures, ±L

Rupture scenarios weighted by expert groups from available data

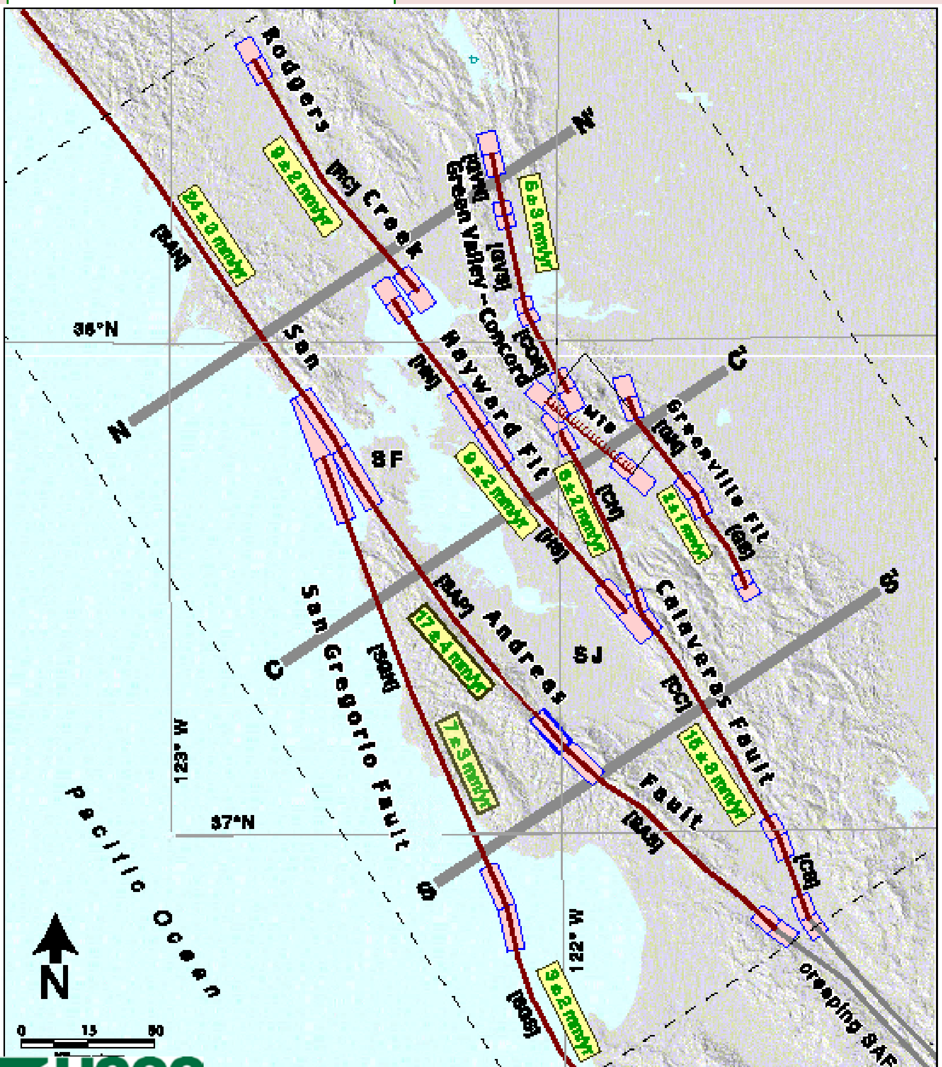

Table 4.8. Long-term magnitudes and occurrence rates of rupture sources. For reference, recurrence intervals are also listed; these are simply calculated as the inverse of the occurrence rate statistics listed in the center columns.

Fault Name	Rupture Source	Mean magnitude: Mean	Mean magnitude: 2.5%	Mean magnitude: 97.5%	Occurrence rate (/yr): Mean	Occurrence rate (/yr): 2.5%	Occurrence rate (/yr): 97.5%	Recurrence interval (yr): Mean	Recurrence interval (yr): 2.5%	Recurrence interval (yr): 97.5%
San Andreas	SAS	7.03	6.84	7.22	0.0007	0	0.0015	1402	646	–
	SAP	7.15	6.95	7.32	0.0005	0	0.0010	2017	967	–
	SAN	7.45	7.28	7.61	0.0001	0	0.0008	7180	1316	–
	SAO	7.29	7.12	7.44	0.0002	0	0.0011	4540	897	–
	SAS+SAP	7.42	7.26	7.56	0.0010	0.0002	0.0029	1037	343	4863
	SAP+SAN	7.65	7.48	7.79	0	0	0	–	–	–
	SAN+SAO	7.70	7.53	7.86	0.0012	0.0004	0.0035	809	282	2772
	SAS+SAP+SAN	7.76	7.59	7.92	0.00002	0	0.0001	42489	8240	–
	SAP+SAN+SAO	7.83	7.65	8.01	0.0001	0	0.0004	13046	2676	–
	SAS+SAP+SAN+SAO	7.90	7.72	8.10	0.0026	0.0012	0.0042	378	239	808
	floating	6.90	6.90	6.90	0.0009	0.0001	0.0019	1104	536	7723
Hayward/RC	HS	6.67	6.36	6.93	0.0034					
	HN	6.49	6.18	6.78	0.0032					
	HS+HN	6.91	6.68	7.12	0.0024					
	RC	6.98	6.81	7.14	0.0040					
	HN+RC	7.11	6.94	7.28	0.0005					
	HS+HN+RC	7.26	7.09	7.42	0.0003					
	floating	6.90	6.90	6.90	0.0003					
Calaveras	CS	5.79	0.00	6.14	0.0075					
	CC	6.23	5.75	6.68	0.0054					
	CS+CC	6.36	5.87	6.75	0.0018					
	CN	6.78	6.58	6.97	0.0035					
	CC+CN	6.90	6.68	7.11	0.0001					
	CS+CC+CN	6.93	6.72	7.14	0.0006					
	floating	6.20	6.20	6.20	0.0030					
	floating CS+CC	6.20	6.20	6.20	0.0120					
Concord/GV	CON	6.25	5.75	6.67	0.0014					
	GVS	6.24	5.75	6.65	0.0007					
	CON+GVS	6.58	6.13	6.91	0.0005					
	GVN	6.02	5.45	6.49	0.0017					
	GVS+GVN	6.48	6.03	6.81	0.0009					
	CON+GVS+GVN	6.71	6.34	7.00	0.0017					
	floating	6.20	6.20	6.20	0.0026					
San Gregorio	SGS	6.96	6.75	7.17	0.0007					
	SGN	7.23	7.04	7.41	0.0012					
	SGS+SGN	7.44	7.27	7.58	0.0008					
	floating	6.90	6.90	6.90	0.0008					
Greenville	GS	6.60	6.37	6.83	0.0010					
	GN	6.66	6.41	6.88	0.0010					
	GS+GN	6.94	6.74	7.13	0.0005					
	floating	6.20	6.20	6.20	0.0002					
Mt Diablo	MTD	6.65	6.42	6.89	0.0026					

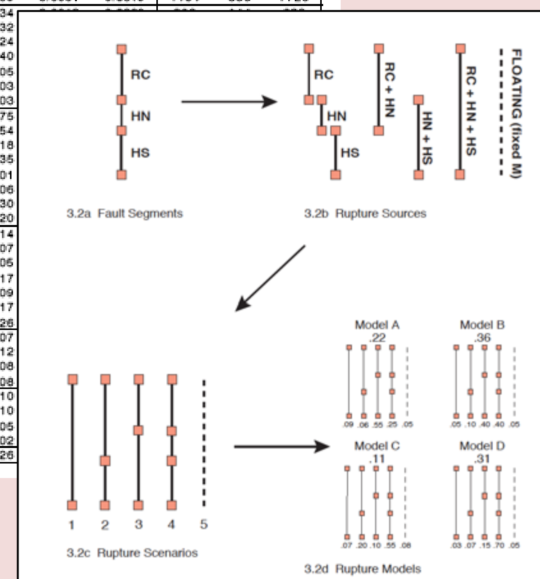

WGUEP 2016

Wasatch Fault Segmentation: Central 5 Segments with Endpoint Uncertainties

- time-stratigraphic OxCal models, slip/event data at 23 sites
- fault geometry

<u>Segment Rupture Lengths</u>

Min: 20-46 km
Max: 41-71 km

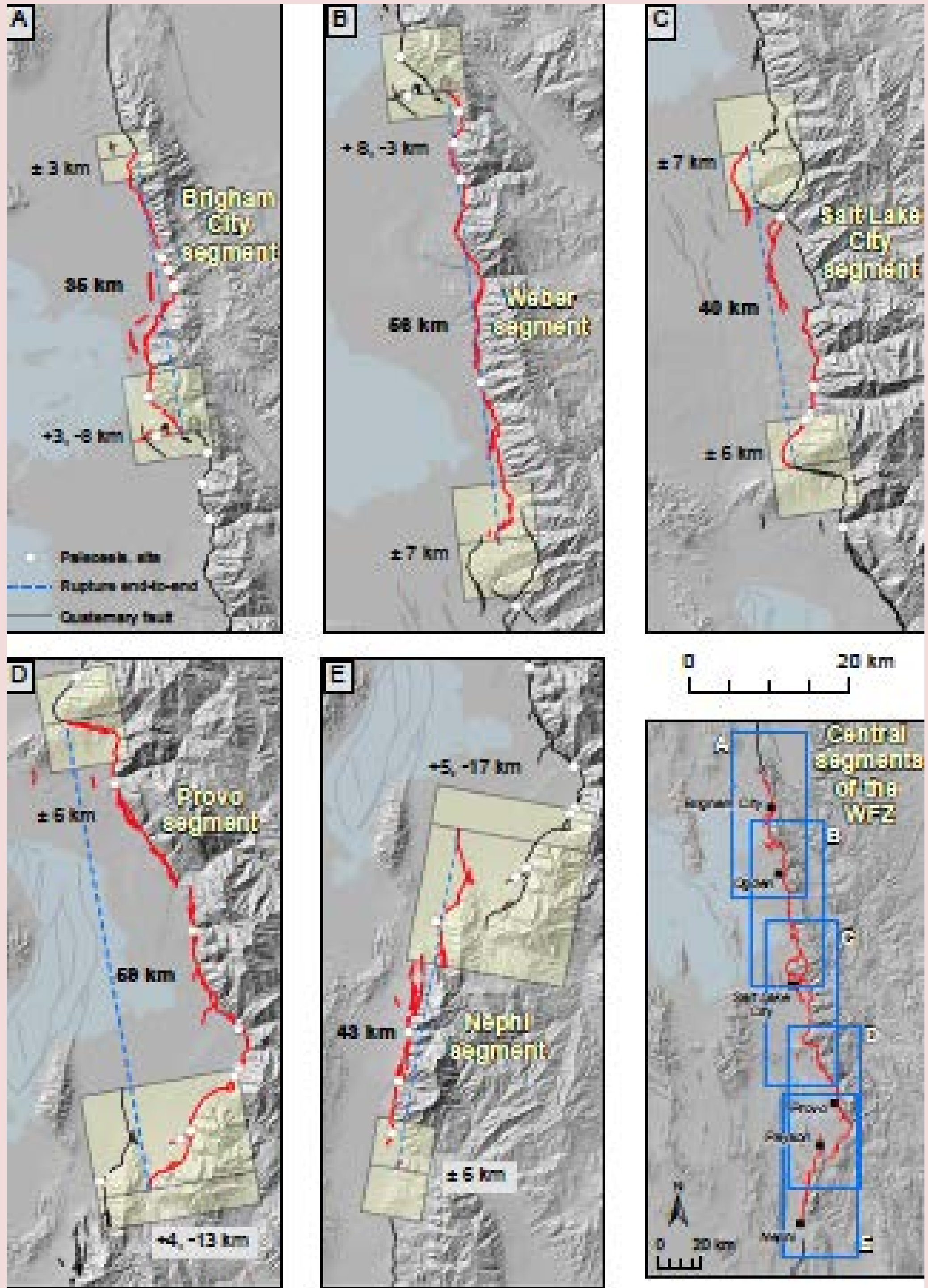

Wasatch Fault Rupture Models with Weights

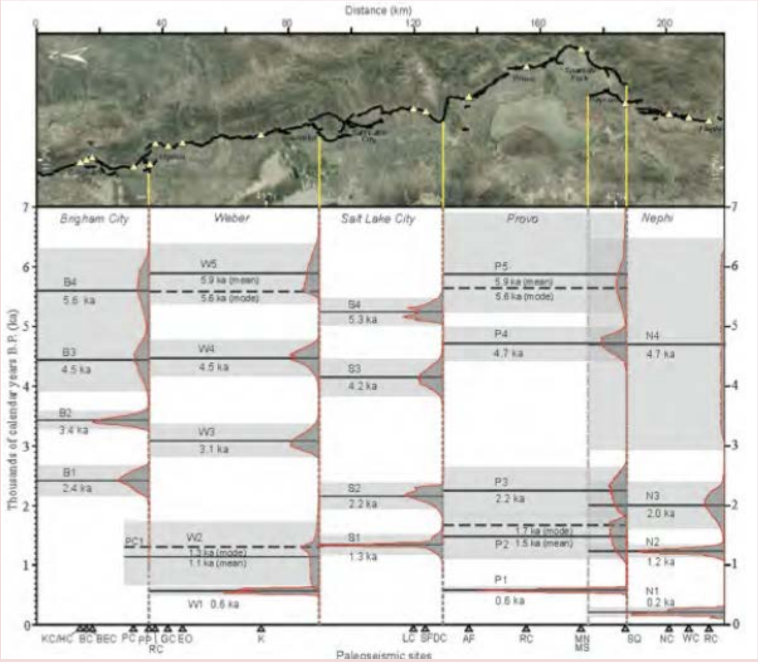

single segment (.7)

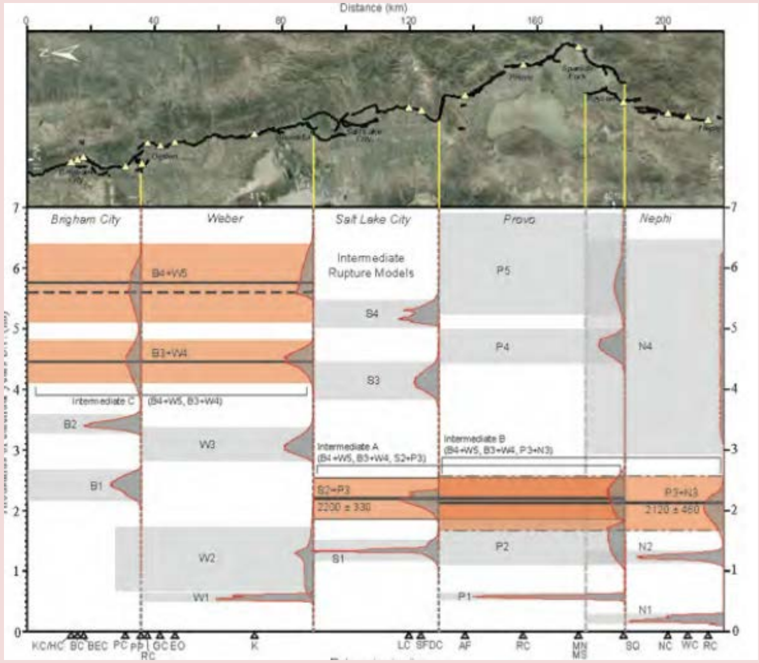

single + multi-segment(.175)

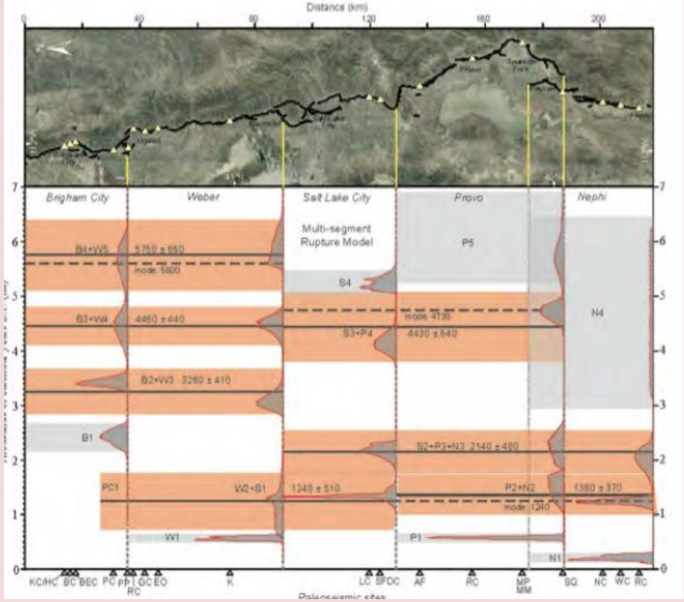

all multi-segment (.025)

WGUEP (2016)

Fault Segmentation: The Controversy

Although WGCEP, 2007, was successful in terms of stated goals, a number of issues were identified in the "Model Limitations and Opportunities for Future Improvements" section of the report. The most salient of these were (1) to relax segmentation assumptions and include multifault ruptures and

dramatically, exemplified following the UCERF2 publication, by events such as the 2011 *M* 9 Tohoku earthquake with respect to segmentation (e.g., Kagan and Jackson, 2013), the 2011 *M* 6.3 Christchurch earthquake in terms of spatiotemporal clustering (e.g., Kaiser *et al.*, 2012), and both the 2010 *M* 7.2 El Mayor–Cucapah and 2012 *M* 8.6 Sumatra earthquakes in regard to multifault ruptures

A persistent problem in WGCEP and NSHMP studies of California seismicity has been the overprediction, or bulge, in the modeled event rates between *M* 6.5 and 7.0 (e.g., the "earthquake deficit" described in WGCEP, 1995). The UCERF2 rates also showed a bulge in this magnitude range, requiring *ad hoc* adjustments to lower them to within the 95% confidence bounds of observed rates. WGCEP, 2007, speculated that the relaxation of strict segmentation would provide a better solution to the bulge problem, and they noted that the multifault ruptures observed in the 1992 Landers, California, and 2002 Denali, Alaska, earthquakes supported this hypothesis

From UCERF 3
Field et al.(2014)

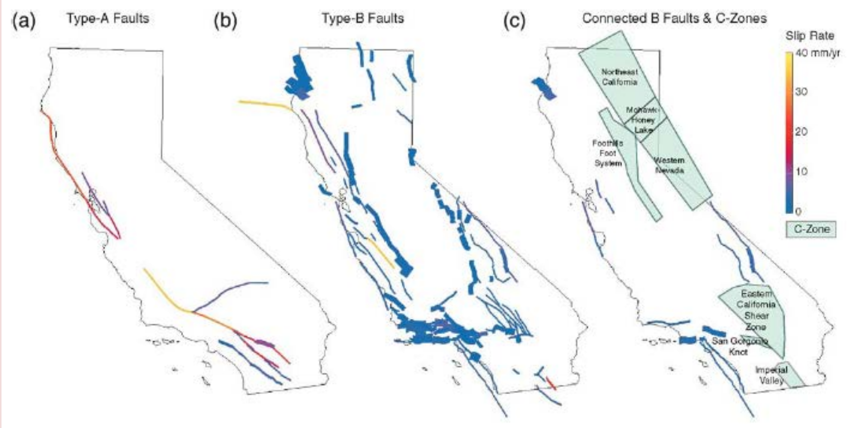

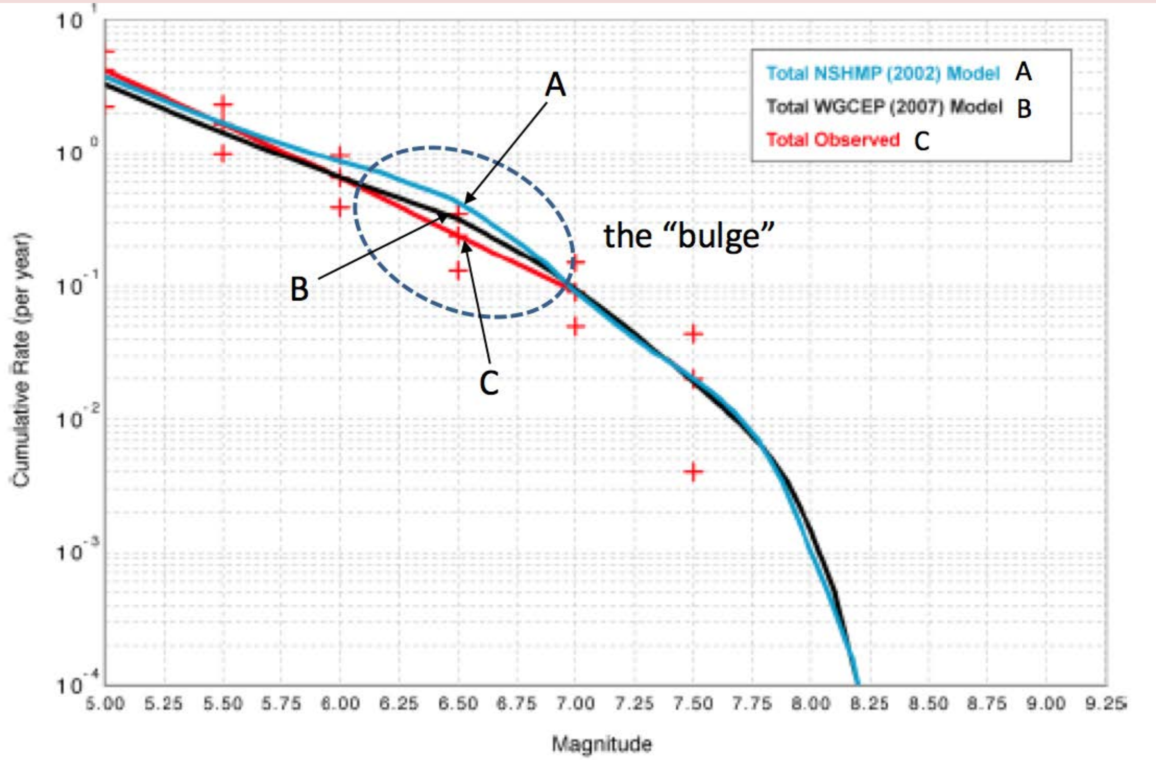

UCERF 2
Field et al. (2009)

UCERF 3 (Field et al., 2014)

Systematic treatment of CA faults

Relax segmentation—fault-to-fault jumps, longer ruptures

Reduce the bulge

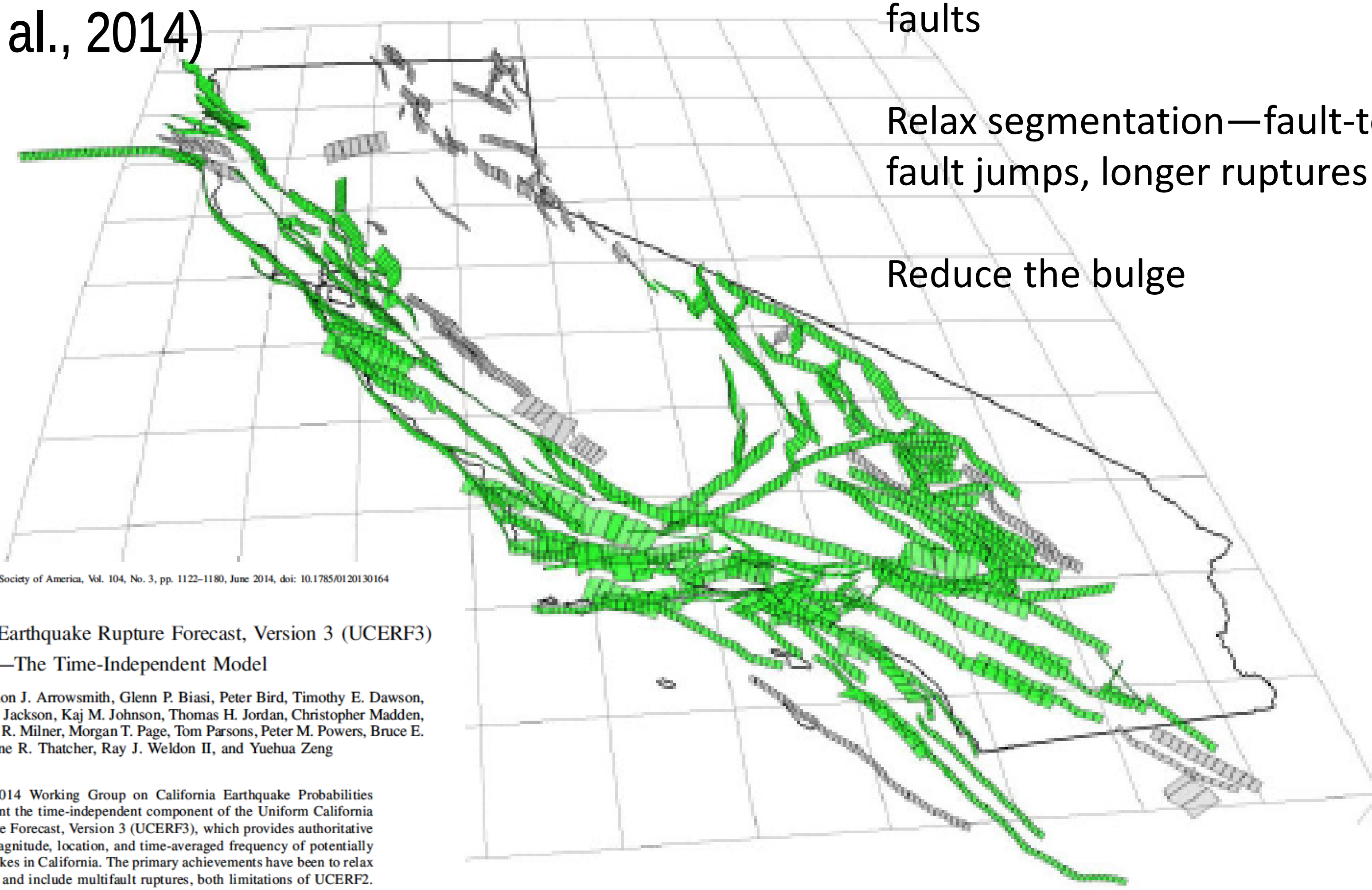

Bulletin of the Seismological Society of America, Vol. 104, No. 3, pp. 1122–1180, June 2014, doi: 10.1785/0120130164

Uniform California Earthquake Rupture Forecast, Version 3 (UCERF3) —The Time-Independent Model

by Edward H. Field, Ramon J. Arrowsmith, Glenn P. Biasi, Peter Bird, Timothy E. Dawson, Karen R. Felzer, David D. Jackson, Kaj M. Johnson, Thomas H. Jordan, Christopher Madden, Andrew J. Michael, Kevin R. Milner, Morgan T. Page, Tom Parsons, Peter M. Powers, Bruce E. Shaw, Wayne R. Thatcher, Ray J. Weldon II, and Yuehua Zeng

Abstract The 2014 Working Group on California Earthquake Probabilities (WGCEP14) present the time-independent component of the Uniform California Earthquake Rupture Forecast, Version 3 (UCERF3), which provides authoritative estimates of the magnitude, location, and time-averaged frequency of potentially damaging earthquakes in California. The primary achievements have been to relax fault segmentation and include multifault ruptures, both limitations of UCERF2. The rates of all earthquakes are solved for simultaneously and from a broader range of data, using a system-level inversion that is both conceptually simple and extensible. The inverse problem is large and underdetermined, so a range of models is sampled using an efficient simulated annealing algorithm. The approach is more derivative than prescriptive (e.g., magnitude–frequency distributions are no longer

Figure 11. Map showing UCERF3 Fault Model 3.1 sections divided into an integral number of equal length subsections (lengths equal to, or just less than, half the section's seismogenic thickness). All subsections shown in green are connected to all others in green without jumping more than 5 km between faults.

USGS science for a changing world

Rupture Rules/Plausibility

Maximum jump distance	5 kilometer
Junction azimuth change	60 degrees
Total azimuth change	60 degrees
Cumulative azimuth change	560 degrees
Cumulative rake change	180 degrees
Minimum number of subsections per fault	2
Coulomb filter	PΔCFF $\geq$ 0.04 or ΔCFF $\geq$ 1.25 bar

Maximum jump distance: 5 km

Coulomb criterion: earthquake triggering is physically reasonable between adjacent sections

Milner et al.(2013)

2606 subsections = 253, 706 ruptures (FM3.1)

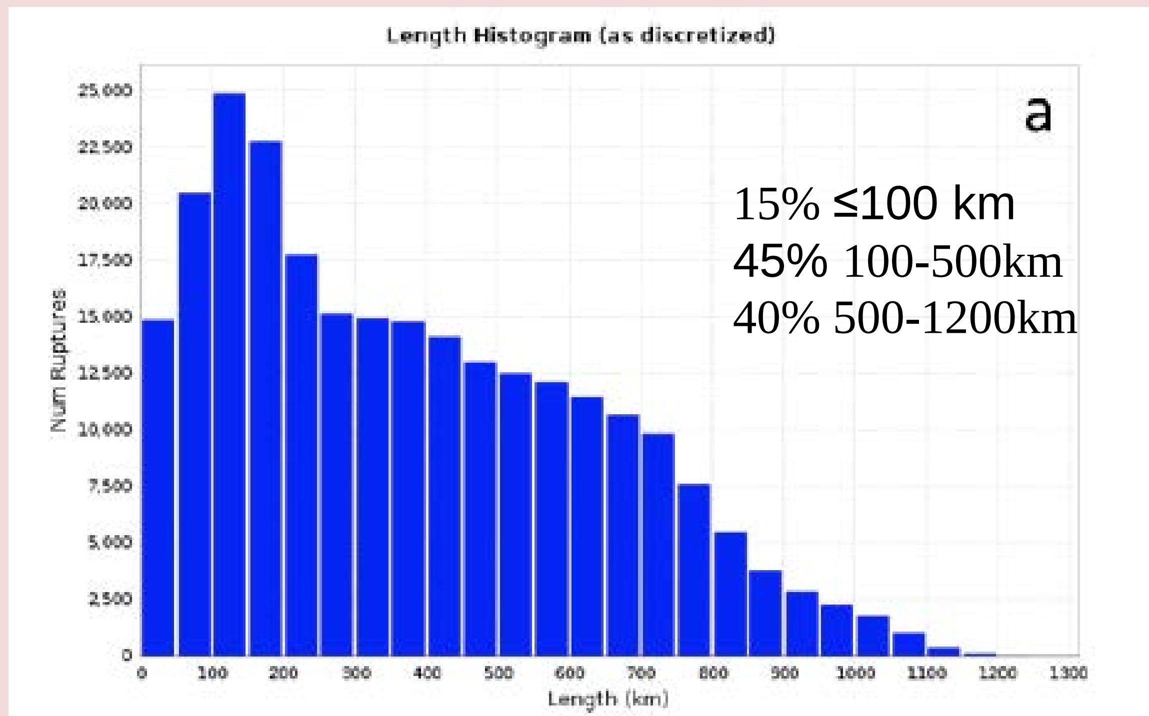

Grand Inversion: Long-term Rates on Fault Ruptures

Field et al. (2014)

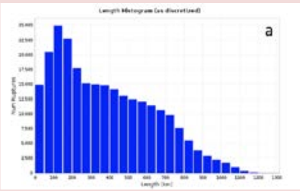

Table 6
The Grand Inversion System of Equations Used in Solving for the Long-Term Rate of Fault-Based Ruptures

Equation Set		Description
$\sum_{r=1}^{R} D_{sr} f_r = v_s$	(1)	**Slip Rate Balancing:** v_s is the subsection slip rate (from a deformation model) and D_{sr} is the slip on the sth subsection in the rth event, averaged over multiple occurrences of the rupture and as measured at midseismogenic depth.
$\sum_{r=1}^{R} G_{sr} P_r^{\text{paleo}} f_r = f_s^{\text{paleo}}$	(2)	**Paleoseismic Event Rate Matching:** f_s^{paleo} is a paleoseismically inferred event rate estimate, G_{sr} specifies whether the rth rupture utilizes the sth subsection (0 or 1), and P_r^{paleo} is the probability that the rth rupture would be seen in a paleoseismic trench.
$R_s^m = \frac{R_{s-1}^m + R_{s+1}^m}{2}$	(3)	**Fault Section Smoothness Constraint:** This enables forcing the nucleation rate, R, in the mth magnitude bin to vary smoothly along a fault section, where the $s-1$ and $s+1$ subsections are adjacent to the sth subsection.
$\lambda_r f_r = 0$	(4)	**Improbability Constraint:** This allows us to force relatively improbable events to have a lower rate (e.g., based on multifault rupture likelihoods). A higher value adds more misfit for a given rupture rate, forcing the inversion to minimize that rupture rate further.
$f_r = f_r^{a\text{-priori}}$	(5)	***a priori* Constraint:** This constrains the rates of particular ruptures to target values, either on an individual basis (e.g., make Parkfield occur every ~25 years) or for a complete rupture set (e.g., as close as possible to those in UCERF2).
$\sum_{r=1}^{R} M_{gr}^m f_r = R_g^m$	(6)	**Regional MFD Constraint:** This enables a geographic region, g, to be forced to have a specified magnitude–frequency distribution (MFD), such as Gutenberg–Richter. R_g^m represents the nucleation rate for the mth magnitude bin in the gth region. Matrix $M_{gr}^m f_r$ contains the product of whether the rth rupture falls in the mth magnitude bin (0 or 1) multiplied by the fraction of that rupture that nucleates in the gth region.
$\sum_{r=1}^{R} M_{sr}^m f_r = R_s^m$	(7)	**Fault Section MFD Constraint:** This enables forcing subsections to have specific nucleation MFDs. R_s^m is the nucleation rate for the mth magnitude bin on the sth subsection. Matrix $M_{sr}^m f_r$ contains the product of whether the rth rupture falls in the mth magnitude bin (0 or 1) multiplied by the fraction of that rupture that nucleates on the sth subsection.

f_r represents the frequency or rate of the rth rupture (what we are solving for). Important implementation details, such as equation-set weighting, are given in Appendix N (Page *et al.*, 2013).

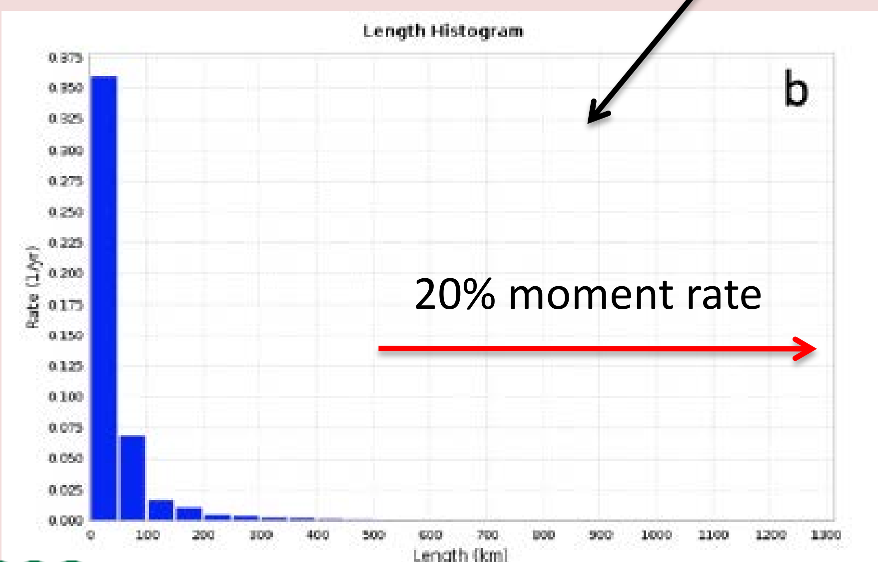

Milner et al. (2013)

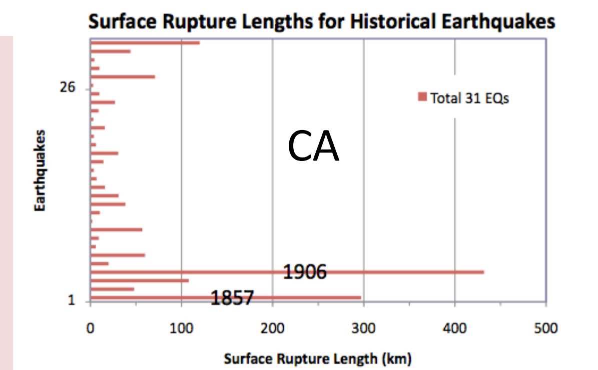

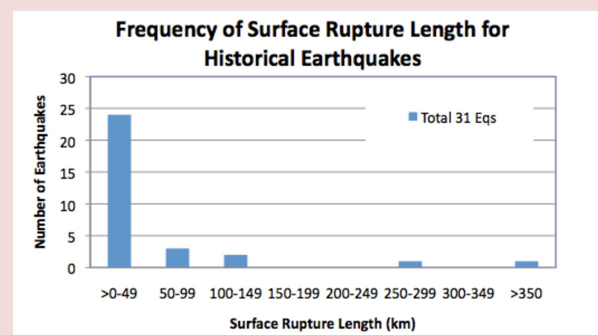

Wells (2013, pc)

Historical Surface Ruptures Worldwide (Shallow Crust) 1848-2014

110 Awatere (1848)
120 Wairapa (1855)
108 Owens Valley (1872) M
101 Pitaycachi (1887) N
115 Tsestserleg (1905)
148 Changma (1932)
120 Luzon (1990)
100 Chi-Chi (1999) T
140 Izmit (1999)
112 Kashmir (2005) T
121 El Mayor (2011)
----
180 FuYun (1931)
180 Bolu (1944)
150 Dari (1947)
----
200 Kirgzia (1911)
220 Haiyuan (1922)
236 Gobi-Altai (1957) M
238 Motagua (1976)
240 Pakistan (2013)
----
280 Kastamonu (1943)
285 Wenchuan (2008) T M
----
350 Fort Tejon (1857)
300 Quingha (1937)
300 Tuosuohi (1963)
341 Denali (2002) 6.2ka
----
370 Bulnay (1905) M
360 Erzincan (1939)
----
470 San Francisco (1906)
410 Kunlun (2001)

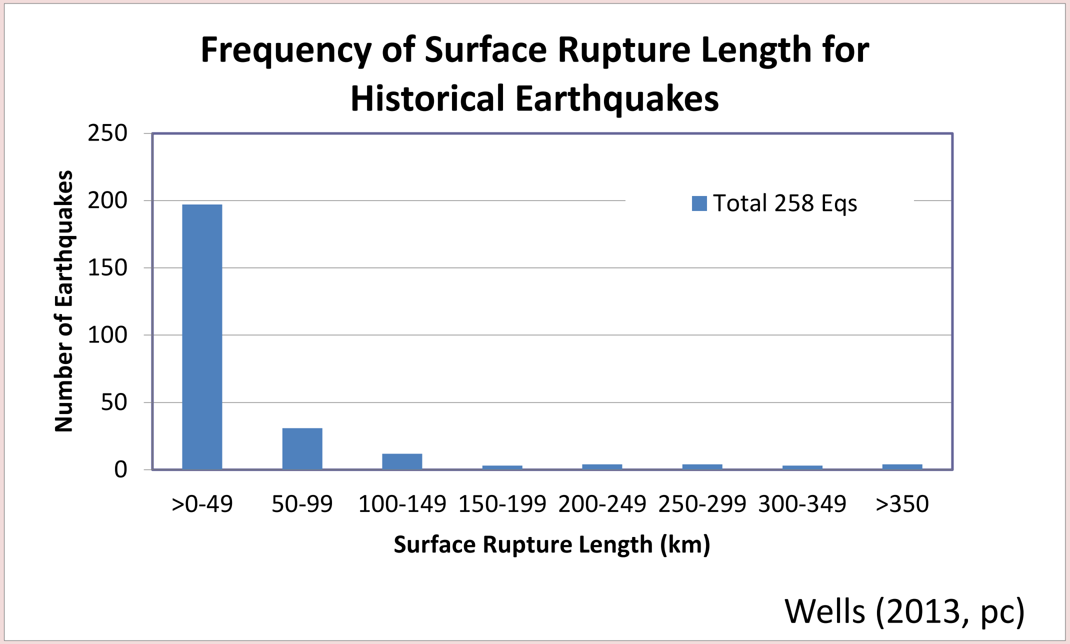

Generally continuous, geomorphically well-defined traces (although not without localized complexity) with limited fault-to-fault jumps or branching; dynamic triggering of associated faults more common

Often represent only partial rupture (~15%-40%) of longer and through going fault zones

USGS science for a changing world

Participation Rate Maps

http://pubs.usgs.gov/of/2013/1165/data/UCERF3_SupplementalFiles/UCERF3.3/Model/FaultParticipation/index.html

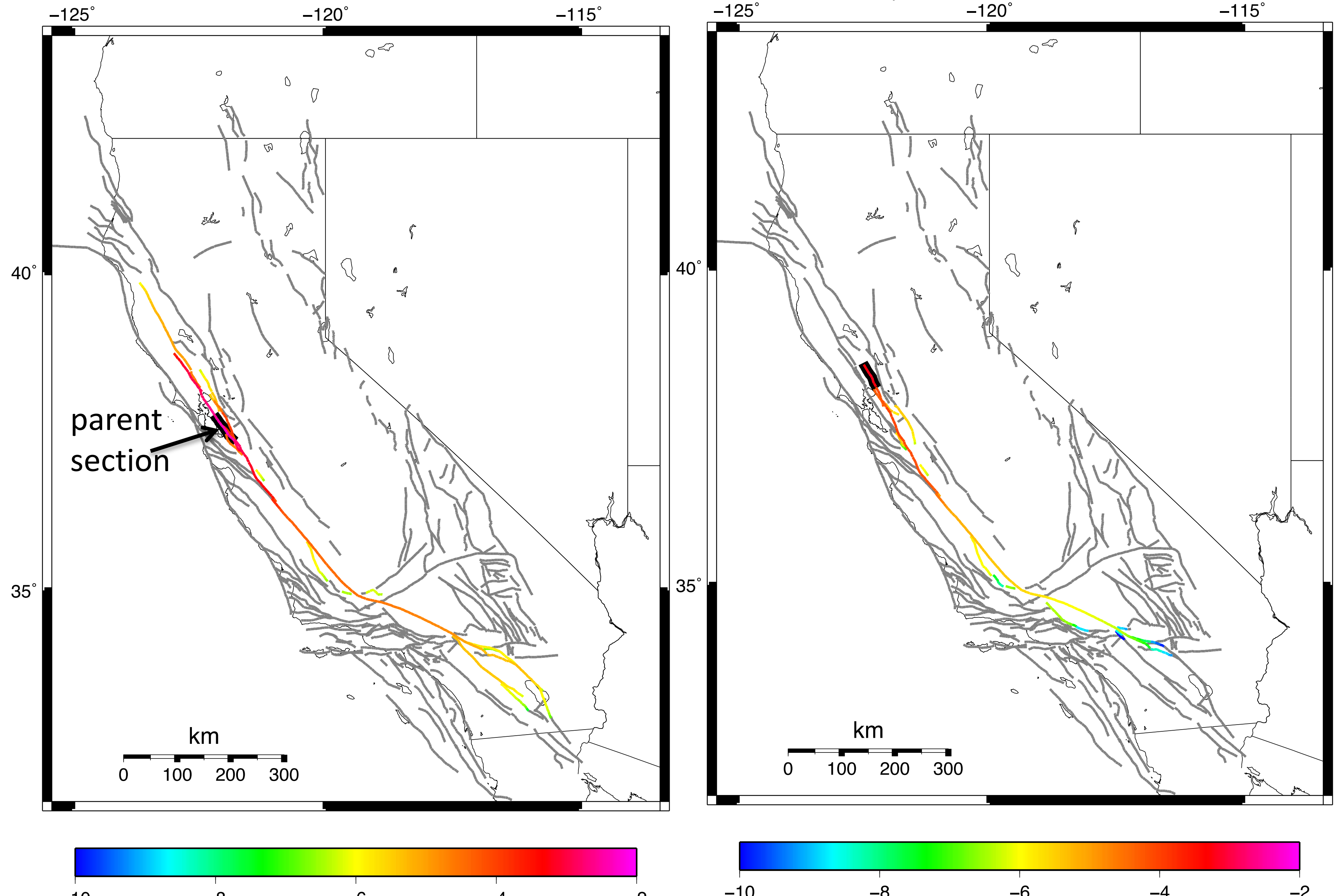

USGS science for a changing world

FM3_1 Hayward (So) 2011 CFM (638)

FM3_1 West Napa 2011 CFM (665)

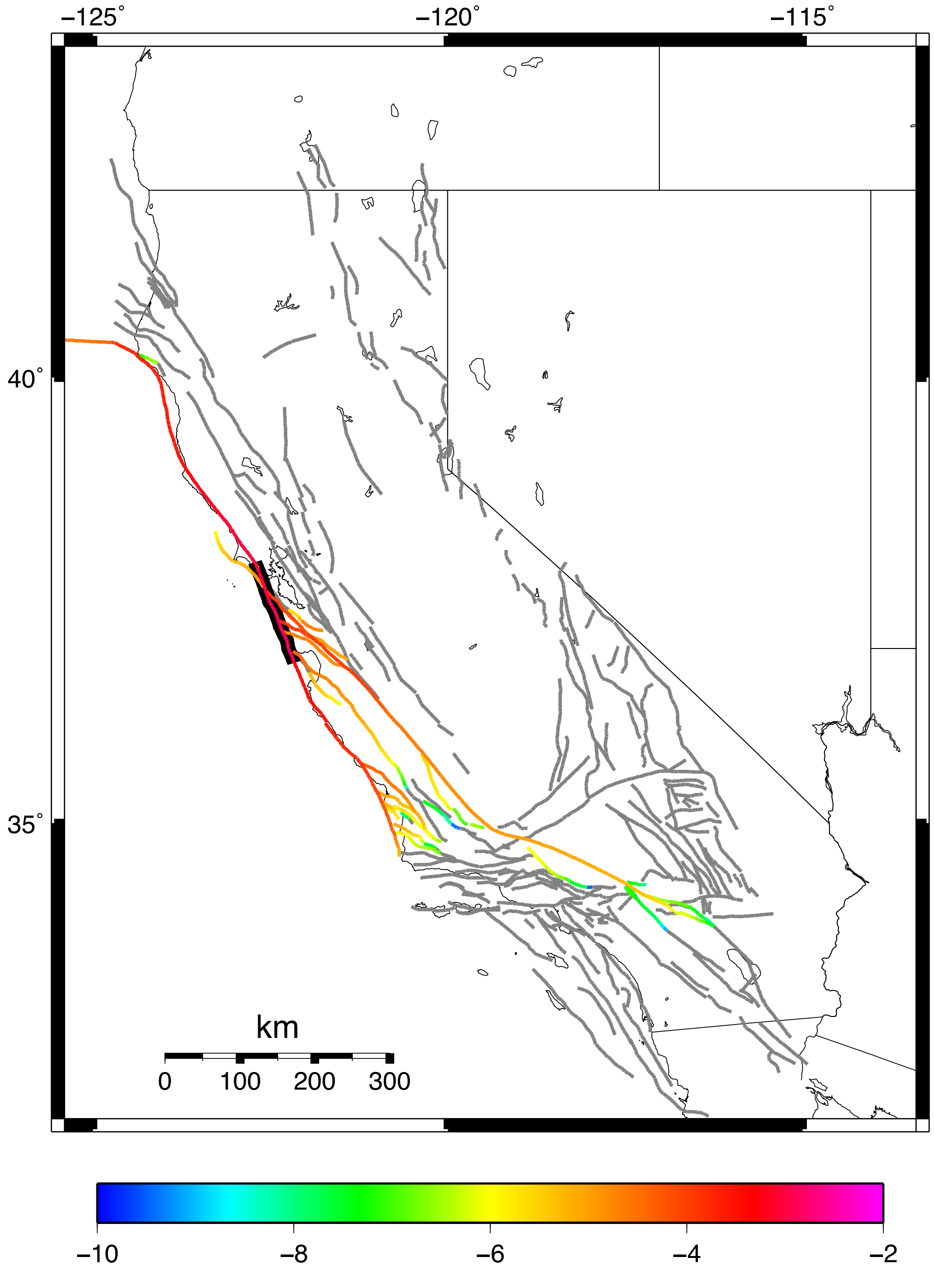

FM3_1 San Gregorio (North) 2011 CFM (660)

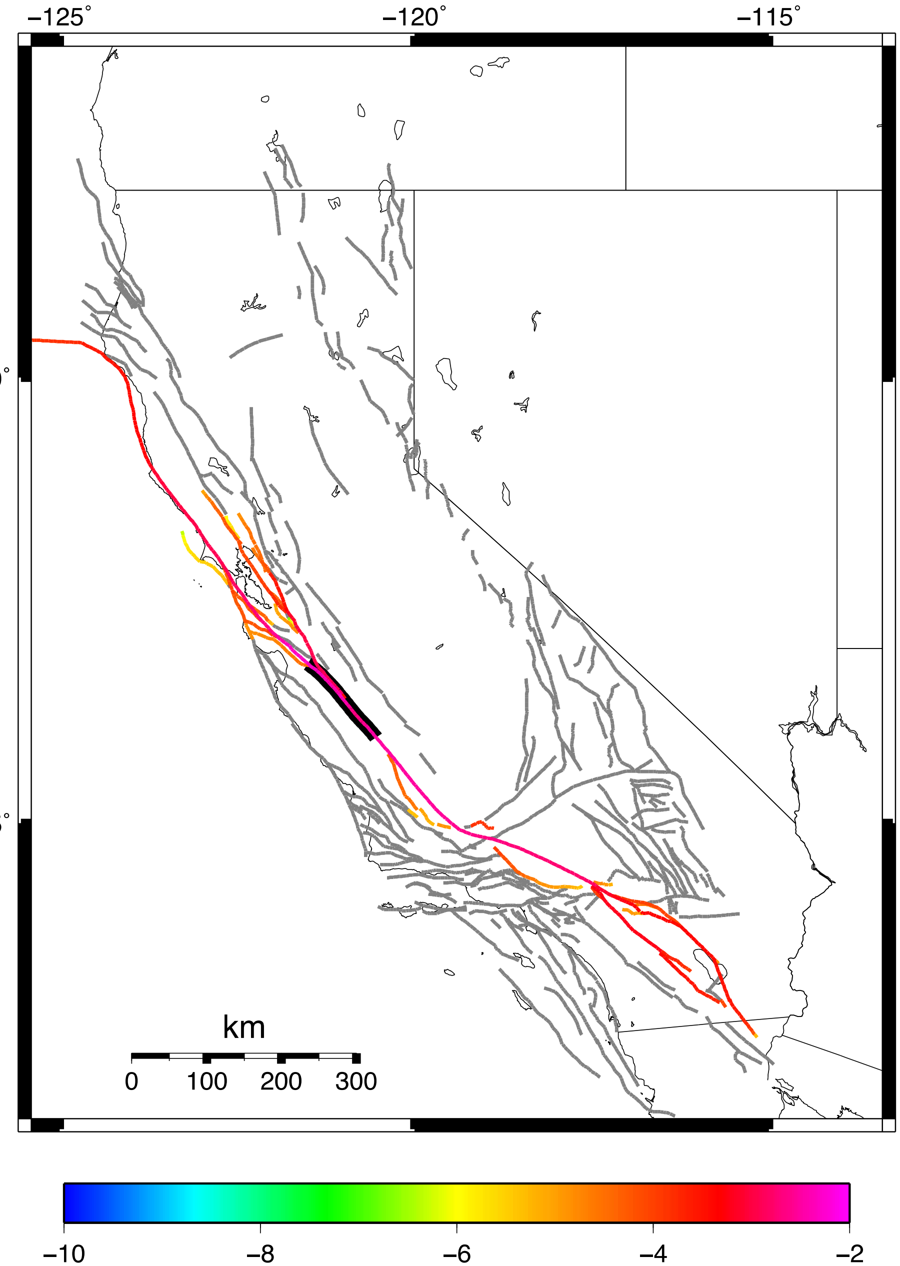

FM3_1 San Andreas (Creeping Section) 2011 CFM (658)

USGS
science for a changing world

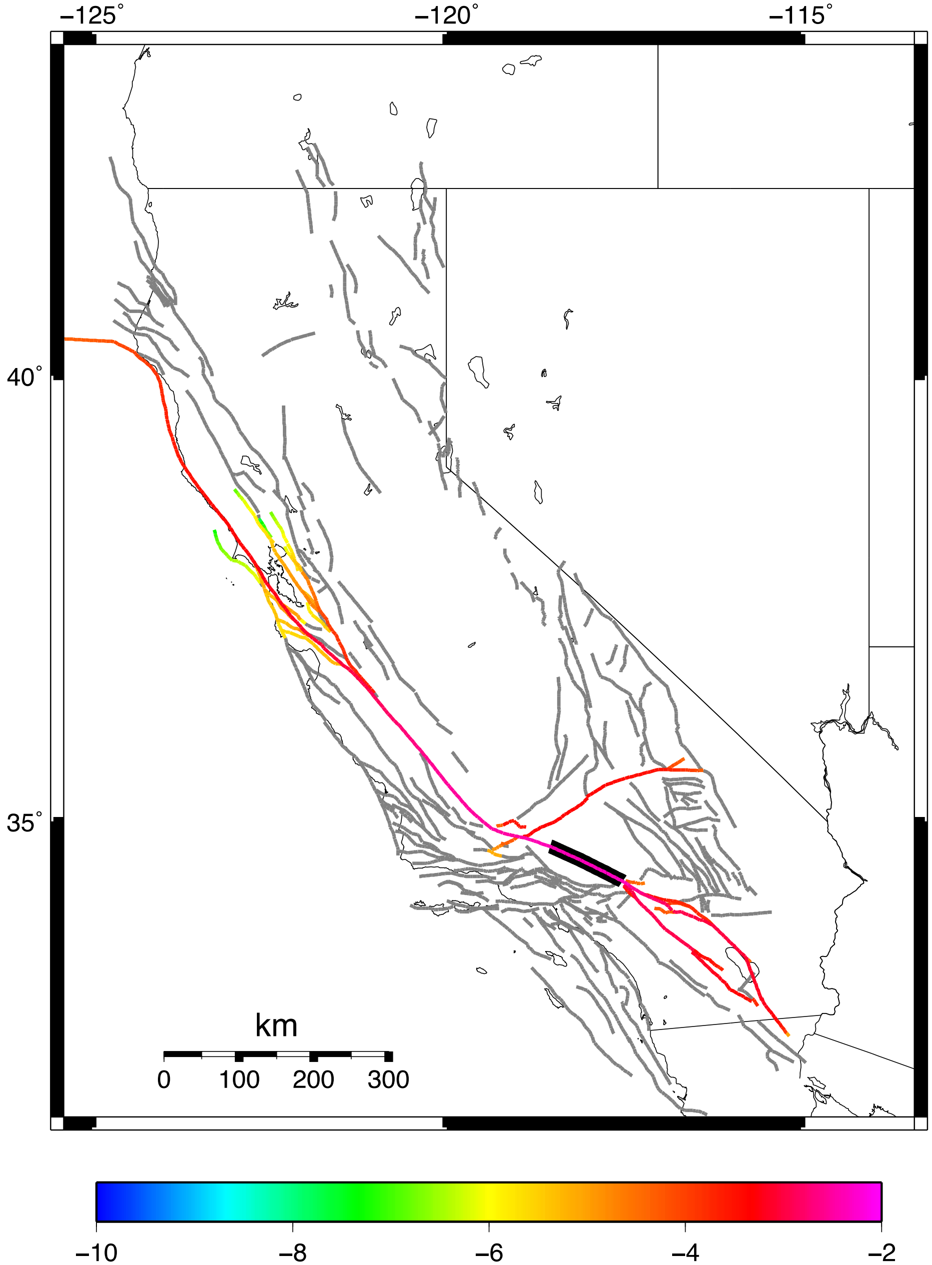

FM3_1 San Andreas (Mojave S) (301)

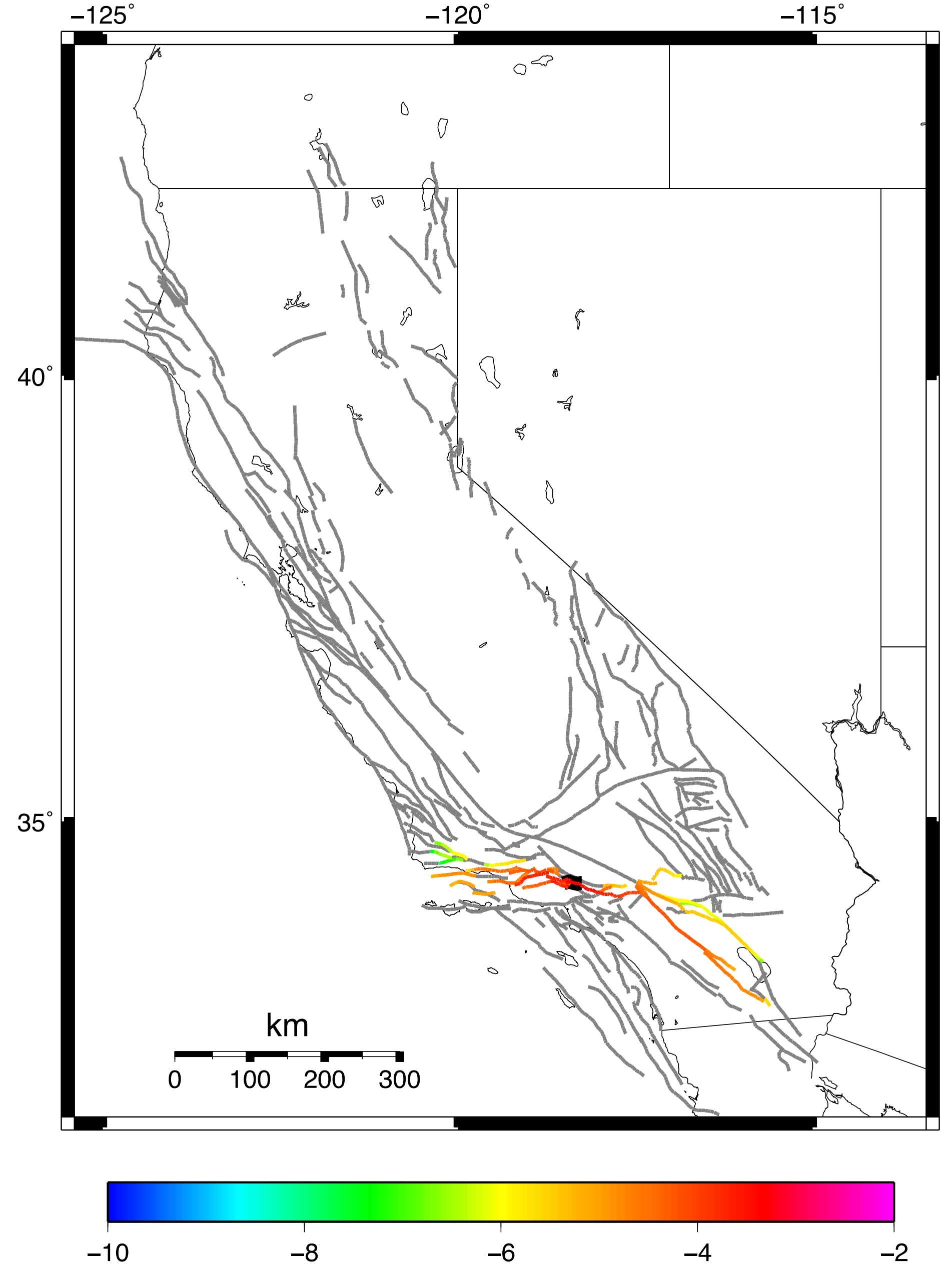

FM3_1 Sierra Madre (San Fernando) (113)

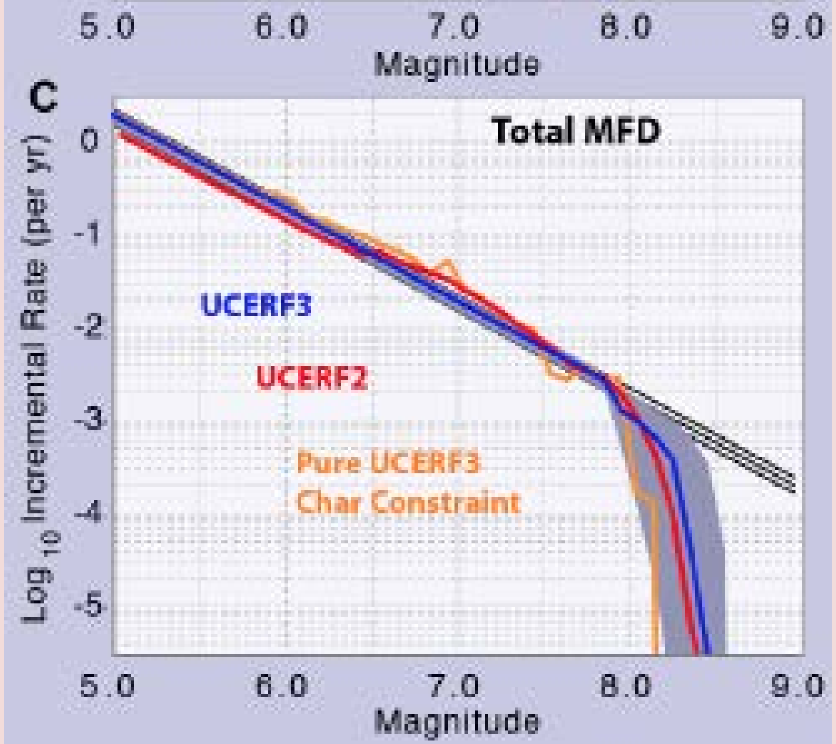

Field et al. (2014)

The Bulge is gone, but…

UCERF 3 PRODUCES TOO MANY UNREALISTICALLY LONG RUPTURES

MODEL OBSCURES THE CONCEPT OF WHAT IS A FAULT? WHAT IS A SOURCE?

USGS science for a changing world

Tales of Denali I: A Retrospective Test of a Segmentation Model

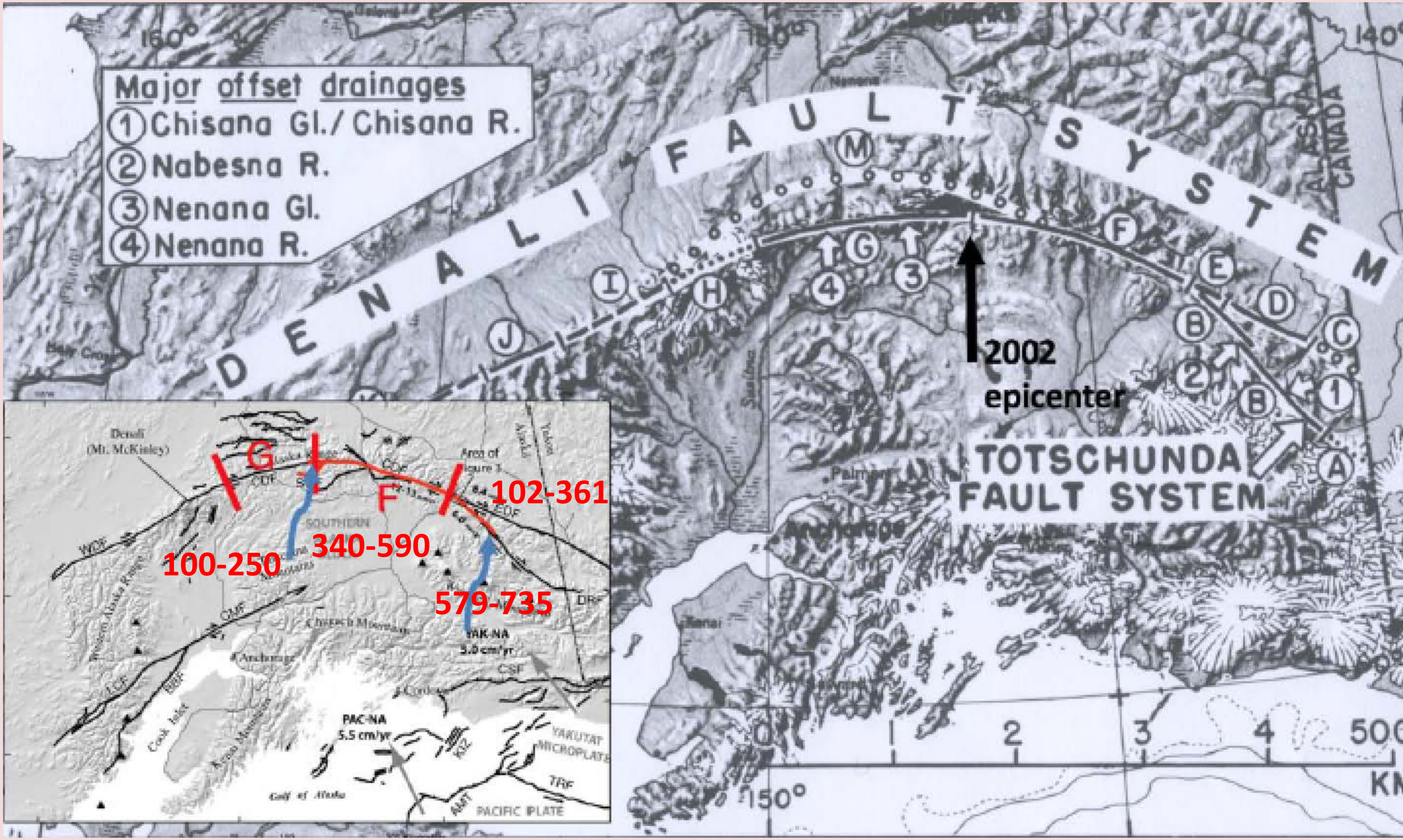

Plafker et al., (1977)

Tales of Denali II:
Controls of Branching—Connectivity, Event Timing, Accumulated Strain

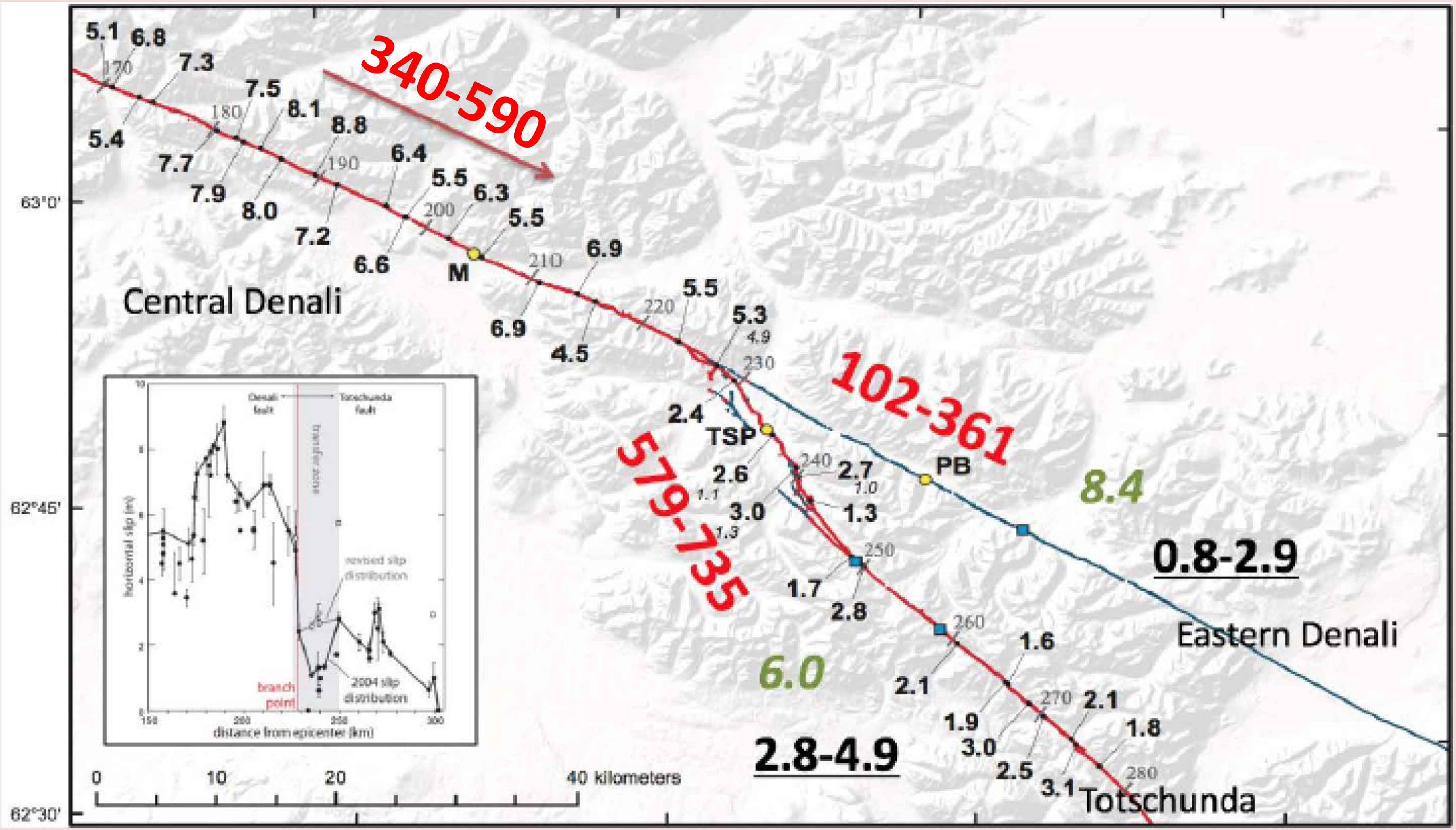

Schwartz et al., (2012)

Some Factors Influencing Fault Rupture Length

- Fault connectivity at depth, and not only a surface separation distance.
- Timing of the most recent prior earthquake(s) along strike (the 2002 Denali to Totschunda);
- Differences in strain accumulation on adjacent fault sections;
- Paleo slip distributions;
- Dynamic rupture including stress effects at branch points or steps;
- Lithological and frictional variability;
- Effects of creep, particularly on dynamic rupture propagation.

Combining these types of data and their interpretations (which can be difficult to obtain) with source-specific behavioral and kinematic observations can lead to effective construction of reasonable rupture models, including single-segment, multi-segment, and multi-fault scenarios for near-future earthquakes of interest (whatever happened to Stringing Pearls?). There is no reason why this cannot be prescribed by expert groups. For many faults under consideration for hazard analysis worldwide, this may be the most effective approach.

Factors Influencing Fault Rupture Length

Connectivity
Geometry: along strike (branching, steps, bends); down-dip (uncertain)

Timing of the prior earthquake(s) along strike (Denali-Totschunda)

Dynamic rupture propagation (requires nucleation location), regional and local stress

Variability in frictional fault properties
Creep, slip-strengthening

Combining information on these with paleoseismic data on the past temporal and spatial behavior of a fault can lead to more effective construction of reasonable rupture models, including single, multi-segment, and multi-fault scenarios for near-future earthquakes. There is no reason why these cannot be prescribed by expert groups. For many faults under consideration for hazard analysis worldwide, this may be the most effective approach